An ab initio determination of the bending–torsion–torsion spectrum of dimethyl ether, CH3OCH3 and CD3OCD3

M. L. Senent, D. C. Moule, and Y. G. Smeyers

Additional information on J. Chem. Phys.

An *ab initio* determination of the bending–torsion–torsion spectrum of dimethyl ether, CH₃OCH₃ and CD₃OCD₃

An *ab initio* determination of the bending–torsion–torsion spectrum of dimethyl ether, CH_3OCH_3 and CD_3OCD_3

M. L. Senent and D. C. Moule
Department of Chemistry, Brock University, St. Catharines, Ontario L2S 3A1, Canada

Y. G. Smeyers
Instituto de Estructura de la Materia, CSIC, c/Serrano, 119, 28006, Madrid, Spain

We have calculated the potential energy hypersurface of dimethyl ether with respect to the COC bending coordinate α and the torsional angles of the two methyl groups, θ_1 and θ_2. Two sets of *ab initio* calculations were carried out. The first was made at the level MP2/6-31G(d,p) in which the structural coordinates were fully relaxed except for the grid points on the hypersurface. More extensive calculation were carried out with MP4 corrections for electron correlation with the same molecular structure. The torsional bending Hamiltonian matrix was symmetrized by the operations of the G_{36} nonrigid group and was solved variationally. The effect of explicitly considering the bending mode in the three-dimensional treatment was determined by a comparison to the two-dimensional model in which the flexibility of the frame was absorbed into the calculation by the fully relaxed method. It was found that the three-dimensional calculation gave a much better account of the $\sin(3\theta_1)\sin(\theta_2)$ intermode coupling than the two-dimensional treatment. © *1995 American Institute of Physics.*

I. INTRODUCTION

Molecules containing interacting methyl groups often have a far infrared torsional band spectrum that is highly congested.[1] One solution to the problem of band assignments of these complex spectra is the direct simulation of the band profiles by the *ab initio* calculations.[2] Such calculations provide information about the shapes of the potential surfaces governing methyl rotation as well as the kinetic interactions between the methyl groups.

The most effective method for accounting for the interactions between the top and the frame is the so-called technique of full relaxation of all structural coordinates.[3] In this method, the structural parameters are optimized during the Hartree–Fock calculation of the total electronic energy except for the torsional angles that form the grid points for the potential surface.

In the specific case of dimethyl ether, DME, the simultaneous rotations of the two methyl groups set up a powerful steric interaction between the adjacent methyl groups that results in a flexing of the central COC bond angle. This interaction between the bending of the COC frame and the rotations of the methyl groups manifests itself in a coupling between the $Q_{15}(b_1)$ and $Q_{11}(a_2)$ torsional modes and the $Q_7(a_1)$ in-plane bending mode. Moreover, as the overtone of the gearing mode, $2\nu_{15}(a_1)$, in DME-h_6 lies at 481.2 cm^{-1} it is in an ideal position for a resonance perturbation with the 412.0 cm^{-1} $\nu_7(a_1)$ COC bending fundamental.

In our earlier study[3] on DME we were unable to account for the localized perturbation between the overtone of the gearing mode and the COC in-plane bending mode by the full relaxation method, even though the levels not directly affected by the perturbation were successfully accounted for. In this article, we extend our model for DME to explicitly include the COC bending as a third large amplitude coordinate. It was anticipated that the introduction of the additional dimension should account for some of the observed perturbations.

II. THEORY

In the equilibrium conformation, ($\theta_1=0$, $\theta_2=0$), the in-plane hydrogens atoms of the two methyl groups of DME are found to eclipse the oxygen atom. Figure 1 shows the equilibrium structure and the symmetry axes. The direction of rotation of the methyl hydrogens are defined in the clockwise sense for both groups. In the rigid approximation, the Q_7 COC in-plane bending mode and the torsions of the methyl groups in the same sense Q_{11} (antigearing) and in the opposite sense Q_{15} (gearing) can be classified by the a_1, a_2, and b_1 representations of the C_{2v} point.

The three-dimensional dynamical model for DME may be classified by the restricted nonrigid group proposed by Smeyers[4] who defines the nonrigid symmetry operations in terms of the internal coordinates. This r-NRG group is identical to the group of symmetry operations that commute with the DME nuclear Hamiltonian when the molecule is described as a two-dimensional system where the variables are the torsional angles. Thus, the symmetry properties of the system are unmodified by the addition of the in-plane bend-
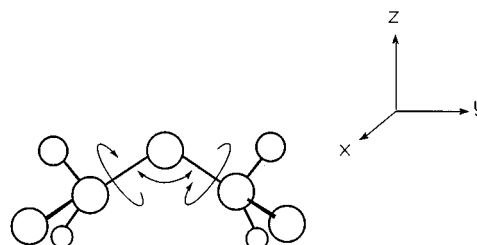

FIG. 1. The equilibrium structure of dimethyl ether, the x, y, and z symmetry axes and the definitions of the θ_1, θ_2, and α torsion and bending coordinates.

ing motion as a third large amplitude coordinate. The r-NRG G_{36} group is defined by the same nonrigid operations that were used in a recent study of acetone.[2(a)] This group has four nondegenerate A_i representations, four two degenerate representations E_i and one four degenerate representation, G.

The a_1, a_2, b_1, and b_2 representations of the C_{2v} point group correlate with the A_1, A_3, A_2, and A_4 singly degenerate representations of the r-NRG G_{36} group.

When only the three lowest frequency modes are considered, the nuclear Hamiltonian for DME may be written as

$$\hat{H}(\alpha,\theta_1,\theta_2) = -B_1(\alpha,\theta_1,\theta_2)\frac{\partial^2}{\partial\theta_1^2} - 2B_{12}(\alpha,\theta_1,\theta_2)\frac{\partial^2}{\partial\theta_1\partial\theta_2} - B_2(\alpha,\theta_1,\theta_2)\frac{\partial^2}{\partial\theta_2^2} - 2B_{13}(\alpha,\theta_1,\theta_2)\frac{\partial^2}{\partial\alpha\partial\theta_1}$$

$$-2B_3(\alpha,\theta_1,\theta_2)\frac{\partial^2}{\partial\alpha^2} - 2B_{23}(\alpha,\theta_1,\theta_2)\frac{\partial^2}{\partial\alpha\partial\theta_2} + V(\alpha,\theta_1,\theta_2), \tag{1}$$

where $B_1(\alpha,\theta_1,\theta_2)$, $B_2(\alpha,\theta_1,\theta_2)$, and $B_3(\alpha,\theta_1,\theta_2)$ are the kinetic energy coefficients for the methyl torsion and the bending coordinates and $B_{12}(\alpha,\theta_1,\theta_2)$, $B_{13}(\alpha,\theta_1,\theta_2)$, and $B_{23}(\alpha,\theta_1,\theta_2)$ are the corresponding interaction parameters. All of these coefficients can be obtained by fitting the values for each nuclear conformation to the A_1 symmetry adapted Fourier series. As the variation in the kinetic parameters are small at bending angles close to the equilibrium position, it was assumed that these parameters are constant. In this case it is possible to neglect the $B_{31}(\alpha,\theta_1,\theta_2)$ and $B_{23}(\alpha,\theta_1,\theta_2)$ kinetic interactions.

The hypersurface selected for the $V(\alpha,\theta_1,\theta_2)$ potential consisted of the bending function, the surface for the two methyl torsions, and their cross coupling terms.

$$V(\alpha,\theta_1,\theta_2) = V^\alpha(\alpha) + V^{cc,ss}(\theta_1,\theta_2) + \sum_M V_M^{\alpha cc,\alpha ss}(\alpha,\theta_1,\theta_2). \tag{2}$$

Over the full range of bending angles, the potential for the bending motion contains two minima. The top of the barrier separating the minima corresponds to the linear COC conformation. As only low quanta of the ν_7(COC) mode are required the asymmetric bending about only one equilibrium position is considered. Figure 2 compares the double well potential for the complete bending coordinate with the one-dimensional potential $V^\alpha(\alpha)$. The analytical form for this anharmonic potential is described by

$$V^\alpha = \sum_{N=1} A_{00N}^{cc}\alpha^N, \tag{3}$$

where the angle α measures the displacement from the equilibrium position. The minimal form for the potential surface for the two torsional angles is an analytical expression of seven terms that transforms as the A_1 representation of the G_{36} group. The complete three-dimensional hypersurface then becomes

$$V(\alpha,\theta_1,\theta_2) = \sum_N \sum_{L>K} \sum_K (A_{KLN}^{cc}\alpha^N[\cos 3K\theta_1 \cos 3L\theta_2 + \cos 3L\theta_1 \cos 3K\theta_2] + A_{KLN}^{ss}\alpha^N[\sin 3K\theta_1 \sin 3L\theta_2$$

$$+ \sin 3L\theta_1 \sin 3K\theta_2]) + \sum_N \sum_K (A_{KKN}^{cc}\alpha^N \cos 3K\theta_1 \cos 3K\theta_2 + A_{KKN}^{ss}\alpha^N \sin 3K\theta_1 \sin 3L\theta_2). \tag{4}$$

The expansion coefficients were determined by fitting Eq. (4) to the total energy data points obtained from the fully optimized *ab initio* calculations.

The nuclear Hamiltonian was solved by the variationally with product harmonic oscillator and free rotor basis functions

$$\Phi(\alpha,\theta_1,\theta_2) = \sum_N \sum_I \sum_J [C_{IJN}^{cc}X_N \cos I\theta_1 \cos J\theta_2$$

$$+ C_{IJN}^{cs}X_N \cos I\theta_1 \sin J\theta_2$$

$$+ C_{IJN}^{sc}X_N \sin I\theta_1 \cos J\theta_2$$

$$+ C_{IJN}^{ss}X_N \sin I\theta_1 \sin J\theta_2], \tag{5}$$

where X_n are the solutions of the harmonic oscillator given by

$$X_N = H_{\gamma\alpha} \exp(-\gamma^2\alpha^2/2). \tag{6}$$

$H_{\gamma\alpha}$ are the Hermite polynomials and γ is

$$\gamma = \frac{A_{002}^{cc}}{B_3}. \tag{7}$$

The double fourier series was symmetry adapted to simplify the diagonalization of the Hamiltonian matrix. The eigenvectors were similar to those employed in the recent analysis of acetone[2a] and were obtained by the application of projection operators onto the solution of the double free rotor. The result of the symmetrization is to block the Hamil-
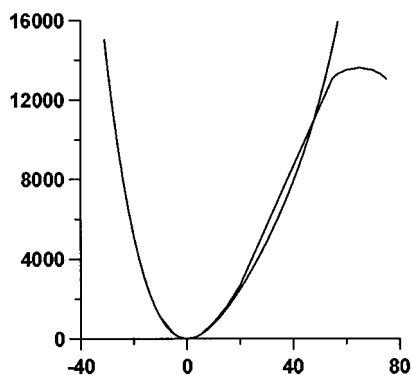
FIG. 2. A comparison of the double well potential for the complete COC bending coordinate with the one-dimensional potential $V^\alpha(\alpha)$.

tonian into 16 boxes corresponding to the nine representations of the G_{36} group. For the levels that lie below the barrier, the internal rotation is restricted and resembles a torsional oscillation that can be described by the quantum num-

bers of the harmonic oscillator. Thus when the torsional splittings are small, the representations of the rigid C_{2v} point group are equally useful in classifying the levels. In this case, each level contains the four microlevels, A_i, E_i, E_i, and G of the G_{36} nonrigid group for a total degeneracy of nine.

Selection rules for the allowed infrared and Raman transitions are identical to those derived for acetone. The intensities of the sharp well-defined c-type bands in the infrared spectrum depend on the x out-of-plane component of the dipole moment. The selection rules are $A_1 - A_2$, $G - G$, $E_1 - E_1$, $E_3 - E_4$, and $G - G$. The Q branches of the bands observed in the Raman spectrum correlate with the diagonal of the polarizability tensor that transforms as the A_1 symmetric representation.

III. COMPUTATIONAL DETAILS

The *ab initio* calculations were performed with the program Gaussian 92.[5] The equilibrium geometry of the ground electronic state was determined from fully optimized calcu-

TABLE I. Relative energies[a] of dimethylether.

			MP2[b]	MP4[b]				MP2[b]	MP4[b]
0	0	0	0.000	0.000	0	0	5	202.398	203.174
60	0	0	1028.077	1006.026	60	0	5	1068.008	1049.898
60	60	0	2132.277	2082.610	60	60	5	1784.008	1745.097
30	0	0	487.304	474.950	30	0	5	611.712	603.044
60	30	0	1559.003	1523.461	60	30	5	1413.649	1386.360
30	30	0	993.608	971.656	30	30	5	1050.545	1033.640
30	−30	0	1011.876	985.612	30	−30	5	943.092	923.312
0	0	1	8.166	8.890	0	0	−5	241.897	241.369
60	0	1	999.995	978.734	60	0	−5	1480.550	1454.686
60	60	1	2013.887	1966.877	60	60	−5	3140.071	3078.276
30	0	1	477.742	467.106	30	0	−5	832.468	818.197
60	30	1	1487.659	1453.784	60	30	−5	2278.008	2235.180
30	30	1	969.727	949.732	30	30	−5	1415.661	1390.106
30	−30	1	956.958	932.008	30	−30	−5	1646.593	1613.709
0	0	−1	9.627	9.707	0	0	10	761.298	762.990
60	0	−1	1075.749	1052.995	60	0	10	1503.315	1490.294
60	60	−1	2277.101	2225.462	60	60	10	1969.570	1942.447
30	0	−1	515.205	503.009	30	0	10	1113.391	1107.440
60	30	−1	1653.319	1616.854	60	30	10	1731.156	1711.270
30	30	−1	1036.278	1014.098	30	30	10	1495.659	1482.514
30	−30	−1	1089.682	1062.283	30	−30	10	1326.290	1312.434
0	0	3	74.265	74.643	0	0	−10	1041.553	1040.652
60	0	3	999.522	979.798	60	0	−10	2539.229	2509.582
60	60	3	1852.218	1809.079	60	60	−10	4930.636	4855.682
30	0	3	511.885	502.162	30	0	−10	1761.070	1744.937
60	30	3	1410.331	1380.181	60	30	−10	3685.505	3634.646
30	30	3	976.398	957.888	30	30	−10	2424.693	2396.004
30	−30	3	910.380	887.316	30	−30	−10	2971.573	2931.865
0	0	−3	85.159	84.803					
60	0	−3	1233.807	1209.187					
60	60	−3	2649.845	2593.457					
30	0	−3	631.088	617.674					
60	30	−3	1914.192	1874.153					
30	30	−3	1182.680	1158.574					
30	−30	−3	1316.982	1286.672					

[a]In cm^{-1}.
[b]The calculations were performed with the 6-31G(d,p) basis set.

TABLE II. Expansion coefficients[a] for the potential energy hypersurface.

	MP2[b]	MP4[b]		MP2[b]	MP4[b]
A_{000}^{cc}	1023.3451	999.8144	A_{202}^{cc}	−0.0011	−0.0009
A_{001}^{cc}	−50.7158	−49.6615	A_{203}^{cc}	0.0001	0.0004
A_{002}^{cc}	10.5104	10.5118	A_{210}^{cc}	1.4655	1.8137
A_{003}^{cc}	−0.1451	−0.1453	A_{211}^{cc}	0.3509	0.3324
A_{100}^{cc}	−534.8878	−522.7965	A_{212}^{cc}	−0.0226	−0.0225
A_{101}^{cc}	32.3620	31.8557	A_{213}^{cc}	0.0007	0.0007
A_{102}^{cc}	−1.0163	−1.0121	A_{220}^{cc}	0.8793	0.7718
A_{103}^{cc}	0.0073	0.0069	A_{221}^{cc}	−0.1523	−0.1528
A_{110}^{cc}	19.1523	17.8470	A_{222}^{cc}	0.0098	0.0087
A_{111}^{cc}	−14.1250	−13.9243	A_{223}^{cc}	0.0000	0.0000
A_{112}^{cc}	0.5814	0.5744	A_{110}^{ss}	−9.3827	−6.9006
A_{113}^{cc}	−0.0050	−0.0048	A_{111}^{ss}	16.5819	16.4074
A_{200}^{cc}	11.0954	11.1987	A_{112}^{ss}	−0.8505	−0.8460
A_{201}^{cc}	−0.5267	−0.5566	A_{113}^{ss}	0.0132	0.0124

[a]In cm^{-1}.
[b]The calculations were performed with the 6-31G(d,p) basis set.

lations within the MP2/6-31G(d,p) approximation. In the equilibrium conformation the in-plane hydrogen atoms were found to eclipse the oxygen atom with a COC bending angle of 110.949°.

The data points that define the three-dimensional potential were obtained from fully optimized calculations at the MP2/6-31G(d,p) and MP4/6-31G(d,p)//MP2/6-31G(d,p) levels. Nine values for the bending angle α range from the equilibrium position, 110.949°, $\alpha=0°$, to $\alpha=\pm10°$. For each value of the bending angle, seven conformations of the torsional coordinates, θ_1 and θ_2 were selected for a total of 49 structures. The data points $(\alpha,\theta_1,\theta_2)$ and the energies relative to the equilibrium position are given in Table I. The energy data points were fitted[6] to Eq. (1) with a standard deviation of 1.035 12 ($R=1.0$) for the MP2 potential and 1.068 40 ($R=1.0$) for the MP4 potential. Table II lists the expansion coefficients for the three-dimensional hypersurface.

The sensitivity of the torsional barriers to the variation of the bending angle is explored in Table III. In the case of the MP4 calculations the height of the barrier increases from 2082.610 cm^{-1} to 3815.030 cm^{-1} when the bending angle is decreased from 0° to −10°. The corresponding increase in bending angle of +10° reduces the barrier to 1179.457 cm^{-1}.

TABLE III. The variation of the torsional barrier[a] with the bending coordinate.

	MP2[b]		MP4[b]	
α	$E_{\alpha,0,60}-E_{\alpha,0,0}$	$E_{\alpha,60,60}-E_{\alpha,0,0}$	$E_{\alpha,60,0}-E_{\alpha,0,0}$	$E_{\alpha,60,60}-E_{\alpha,0,0}$
−10	1497.676	3889.083	1468.930	3815.030
−5	1238.653	2898.174	1213.317	2836.907
−3	1148.648	2508.654	1124.384	2508.654
−1	1066.122	2267.474	1043.288	2215.755
0	1028.077	2132.277	1006.026	2082.610
1	991.829	2005.721	969.844	1957.987
3	925.257	1777.953	905.155	1734.436
5	865.610	1581.610	846.724	1541.923
10	742.017	1208.272	727.304	1179.457

[a]In cm^{-1}.
[b]The calculations were performed with the 6-31G(d,p) basis set.

These trends are to be expected since in the limiting linear COC case, the barrier to methyl rotation is vanishingly small.

The kinetic parameters in the Hamiltonian were determined from the numerical derivatives of the nuclear Cartesian coordinates with respect to the internal coordinates at the equilibrium geometry. The calculated values for DME-h_6 were $B_1(\alpha,\theta_1,\theta_2)=B_2(\alpha,\theta_1,\theta_2)=6.775$, $B_3(\alpha,\theta_1,\theta_2)=1.6508$, and $B_{12}(\alpha,\theta_1,\theta_2)=-1.2402$ cm^{-1} and for DME-d_6, 3.8277, 1.2836, and −0.9990 cm^{-1}. These values are in reasonable agreement with the parameters obtained from microwave spectroscopy:[7] DME-h_6; 6.782 and −1.369 cm^{-1} and for DME-d_6; 3.869 and −1.112 cm^{-1}.

When the Hamiltonian is solved variationally, the accuracy required for convergence of the lower levels requires a basis consisting of 37×37 products of the trigonometric functions and 13 harmonic oscillators for an overall dimension of 37×37×13=17,797. On factorization, the dimensions of the individual boxes reduce to $A_1(637)$; $A_2(546)$; $A_3(546)$; $A_4(468)$; $E_1(2\times1014)$; $E_2(2\times858)$; $E_3(2\times1014)$; $E_4(2\times858)$; $g(4\times2028)$. The matrices were diagonalized with a Givens–Husseldorf routine. Tables IV(a) and IV(b) give the calculated values of the torsion-bending levels classified according to the representations of the G_{36} group. The correspondence between the levels and the quantum numbers for bending were established from the contributions of the harmonic oscillator solutions to the nuclear wave functions. The assignment of the quantum numbers to the excited torsional levels was made from the symmetries of the wave functions. The observed and calculated frequencies of the far infrared bands for DME-h_6 and -d_6 are given in Tables V(a) and V(b).

IV. DISCUSSION

The most dramatic effect of the flexibility of the COC angle on the torsional motion is its influence on the heights of the barriers to methyl rotation. Figure 3 shows a plot of the barrier height, $V(60°,60°)-V(0°,0°)$, and saddle point, $V(60°,0°)-V(0°,0°)$, as function of the COC angle. What is clear is that both the maxima and the saddle points

TABLE IV. (a) Dimethylether-h_6 and (b) dimethylether-d_6 energy levels.[a]

v	v'	v'' [c]		MP2[b]	MP4[b]	v	v'	v''		MP2[b]	MP4[b]
(a)											
0	0	0	A_1	449.009	446.586	0	0	1	A_1	879.688	876.019
			G	449.010	446.586				G	879.688	876.021
			E_1	449.401	446.586				E_1	879.689	876.023
			E_3	449.401	446.586				E_3	879.689	876.023
1	0	0	A_3	651.096	646.085	1	0	1	A_3	1077.971	1070.590
			G	651.091	646.080				G	1077.921	1070.483
			E_2	651.086	646.074				E_2	1077.860	1070.358
			E_3	651.086	646.074				E_3	1077.860	1070.358
0	1	0	A_2	694.193	687.806	0	1	1	A_2	1110.002	1101.482
			G	694.188	687.800				G	1110.010	1101.486
			E_1	694.183	687.795				E_1	1110.025	1101.505
			E_4	694.183	687.795				E_4	1110.025	1101.506
2	0	0	A_1	846.972	839.812	2	0	1	A_1	1286.643	1279.290
			G	847.038	839.887				G	1286.442	1280.026
			E_1	847.105	839.963				E_1	1288.563	1280.778
			E_3	847.105	839.963				E_3	1288.534	1280.740
1	1	0	A_4	880.622	872.174	1	1	1	A_4	1337.995	1327.528
			G	880.736	872.302				G	1337.298	1328.052
			E_2	880.850	872.431				E_2	1343.829	1332.582
			E_4	880.850	872.431				E_4	1344.271	1332.831
0	2	0	A_1	936.104	927.436	0	2	1	A_1	1431.441	1398.712
			G	936.143	927.478				G	1431.143	1399.306
			E_1	936.181	927.519				E_1	1411.642	1400.117
			E_3	936.181	927.519				E_3	1412.660	1400.813
3	0	0	A_3	1034.142	1024.940						
			G	1033.430	1024.131						
			E_2	1032.779	1023.401						
			E_3	1032.779	1023.401						
2	1	0	A_2	1058.714	1048.322						
			G	1057.448	1046.922						
			E_1	1056.148	1045.474						
			E_4	1056.148	1045.475						
1	2	0	A_3	1112.294	1103.209						
			G	1111.664	1102.590						
			E_2	1111.015	1101.946						
			E_3	1111.013	1101.944						
0	3	0	A_2	1175.331	1165.064						
			G	1175.206	1164.934						
			E_1	1175.076	1164.797						
			E_4	1175.090	1164.814						
(b)											
0	0	0	A_1	366.594	364.490	0	0	1	A_1	765.255	761.217
			G	366.594	364.490				G	765.258	761.219
			E_1	366.594	364.490				E_1	765.262	761.221
			E_3	366.594	364.490				E_3	765.262	761.221
1	0	0	A_3	512.753	509.062	1	0	1	A_3	905.314	900.784
			G	512.756	509.065				G	905.325	900.791
			E_2	512.760	509.068				E_2	905.336	900.798
			E_3	512.760	509.068				E_3	905.336	900.798
0	1	0	A_2	559.893	554.940	0	1	1	A_2	964.406	958.037
			G	559.896	554.942				G	964.412	958.041
			E_1	559.898	554.943				E_1	964.417	958.045
			E_4	559.898	554.943				E_4	964.411	958.045
2	0	0	A_1	656.850	651.581	2	0	1	A_1	1045.640	1040.147
			G	656.870	651.598				G	1045.698	1040.198
			E_1	656.890	651.616				E_1	1045.756	1040.248
			E_3	656.890	651.616				E_3	1045.756	1040.248

TABLE IV. (*Continued.*)

v	v'	v'' c		MP2[b]	MP4[b]	v	v'	v''		MP2[b]	MP4[b]
1	1	0	A_4	698.345	691.909	1	1	1	A_4	1096.421	1089.227
			G	698.367	691.928				G	1096.486	1089.286
			E_2	698.389	691.948				E_2	1096.549	1089.343
			E_4	698.389	691.948				E_4	1096.554	1089.348
0	2	0	A_1	734.657	729.156	0	2	1	A_1	1166.888	1160.552
			G	734.663	729.162				G	1166.911	1160.350
			E_1	734.668	729.167				E_1	1166.933	1160.376
			E_3	734.668	729.167				E_3	1166.933	1160.376
3	0	0	A_3	798.072	791.226						
			G	798.149	791.292						
			E_2	798.227	791.358						
			E_3	798.227	791.358						
2	1	0	A_2	833.439	825.497						
			G	833.534	825.575						
			E_1	833.628	825.654						
			E_4	833.628	825.654						
1	2	0	A_3	870.282	862.307						
			G	870.329	862.347						
			E_2	870.376	862.387						
			E_3	870.376	862.387						
0	3	0	A_2	910.833	902.411						
			G	910.849	902.425						
			E_1	910.865	902.439						
			E_4	910.865	902.439						

[a]In cm^{-1}.
[b]6-31G(d,p) basis set.
[c]v, v' and v'' are quantum numbers for the b_1, a_2, and a_1 modes.

are very sensitive to the value of the COC angle. When the angle of the COC group closes the two methyl groups come into each other proximity, and the steric repulsion between the hydrogen atoms increases. On the other hand, as the COC angle opens, the barrier maxima and saddle points decrease. At the linear 180° conformation the methyl groups essentially undergo free rotation.

The major complication in the two top problem involves the description of the $\sin(3\theta_1)\sin(3\theta_2)$ and $\cos(3\theta_1)\cos(3\theta_2)$ coupling terms. The affect of the flexibility of the frame on these terms can be understood from Fig. 4. This is a plot of the A^{ss} and A^{cc} terms as a function of the displacement of the COC bending angle α from its equilibrium position. The explanation of A^{ss} plot is straightforward. As the COC bond angle closes the methyl groups begin to crowd together and hydrogens from the two methyl groups undergo a steric repulsion. For angles less than the equilibrium value, 110.949°, the gearing coupling through the $\sin(3\theta_1)\sin(3\theta_2)$ term is negative and is similar to the well-known case of acetone.[2a] As the COC bond angle opens the A^{ss} term passes through zero near the equilibrium value and changes sign. The positive coupling for larger COC angles is believed to result from an attractive interaction between the electron density on the oxygen and the in-plane eclipsed hydrogen atoms.[8] The $A^{cc}\cos(3\theta_1)\cos(3\theta_2)$ terms are interpreted as an average coupling between the methyl groups. The reduction of this coupling as the COC frame becomes more linear is to be expected. In the case of the three-dimensional calculation, the

variation between the change in coupling with changing COC angle is explicitly taken into account. The two-dimensional calculation, on the other hand, requires that the variation of the coupling terms be absorbed into the dynamical model by the relaxation process.

A direct comparison of the results of the three-dimensional calculation given in Tables V(a) and V(b) with those recently obtained for the fully relaxed model in two dimensions gives an indication of the improvement that can be expected by more extensive treatment. Calculations at the level MP2/6-31G(d,p) for the ν_{15} gearing fundamental $(0,0,0) \rightarrow (0,1,0)$ in two dimensions gives 238.32 cm^{-1} whereas the three-dimensional calculation yields 245.17 cm^{-1}. The observed value is 241.0 cm^{-1}. For the $(0,0,0) \rightarrow (1,0,0)$ antigearing mode, ν_{11}, the value in two dimensions is 207.94 cm^{-1} and 202.081 for three dimensions. An experimental value for this transition is obtained from the weak band at 200.7 cm^{-1} observed by Groner and Durig.[9] Provided the kinetic energy coupling term is small, the difference in frequency between the gearing and antigearing modes is controlled by the $\sin(3\theta_1)\sin(\theta_2)$ coupling term. The observed $\nu_{15} - \nu_{11}$ difference is 40.3 cm^{-1} and is to be compared to the differences for the two- and three-dimensional cases of 30.38 and 43.08 cm^{-1}. Thus, while the three-dimensional model gives a satisfactory description of the interaction, only about 70% of the effect is accounted for by the two-dimensional model. The conclusion that can be drawn from this aspect of the work is that the full relaxation

TABLE V. (a) The frequencies[a] for dimethylether-h_6 and (b) dimethylether-d_6.

$v\ v'\ v''\rightarrow v\ v'\ v''$[c]		MP2[b]	MP4[b]	Obs.
(a)				
$0\ 0\ 0\rightarrow 0\ 1\ 0$	$A_1\rightarrow A_2$	245.184	241.220	
	$G\rightarrow G$	245.178	241.214	241.0
	$E_1\rightarrow E_1$	244.782	241.209	
	$E_3\rightarrow E_4$	244.782	241.209	
$0\ 1\ 0\rightarrow 0\ 2\ 0$	$A_2\rightarrow A_1$	241.911	239.630	
	$G\rightarrow G$	241.955	239.678	240.2
	$E_1\rightarrow E_1$	241.998	239.724	
	$E_4\rightarrow E_3$	241.998	239.724	
$0\ 2\ 0\rightarrow 0\ 3\ 0$	$A_1\rightarrow A_2$	239.227	237.628	
	$G\rightarrow G$	239.063	237.456	238.9
	$E_1\rightarrow E_1$	238.895	237.278	
	$E_3\rightarrow E_4$	238.909	237.295	
$1\ 0\ 0\rightarrow 1\ 1\ 0$	$A_3\rightarrow A_4$	229.526	226.089	
	$G\rightarrow G$	229.645	226.222	223.1
	$E_2\rightarrow E_2$	229.764	226.357	
	$E_4\rightarrow E_4$	229.764	226.357	
$1\ 1\ 0\rightarrow 2\ 1\ 0$	$A_4\rightarrow A_3$	231.672	231.035	
	$G\rightarrow G$	230.928	230.288	225.5
	$E_2\rightarrow E_2$	230.165	229.515	
	$E_4\rightarrow E_4$	230.163	229.514	
$0\ 0\ 0\rightarrow 0\ 0\ 1$	$A_1\rightarrow A_1$	430.679	429.433	
	$G\rightarrow G$	430.678	429.435	412.0
	$E_1\rightarrow E_1$	430.288	429.437	
	$E_3\rightarrow E_3$	430.288	429.437	
$0\ 0\ 1\rightarrow 0\ 1\ 1$	$A_1\rightarrow A_2$	230.314	225.463	
	$G\rightarrow G$	230.322	225.465	224.8
	$E_1\rightarrow E_1$	230.336	225.482	
	$E_3\rightarrow E_4$	230.336	225.483	
(b)				
$0\ 0\ 0\rightarrow 0\ 1\ 0$	$A_1\rightarrow A_2$	193.299	190.450	
	$G\rightarrow G$	193.302	190.452	188.6
	$E_1\rightarrow E_1$	193.304	190.453	
	$E_3\rightarrow E_4$	193.304	190.453	
$0\ 1\ 0\rightarrow 0\ 2\ 0$	$A_2\rightarrow A_1$	174.764	174.216	
	$G\rightarrow G$	174.767	174.220	174.1
	$E_1\rightarrow E_1$	174.770	174.224	
	$E_4\rightarrow E_3$	174.770	174.224	
$0\ 2\ 0\rightarrow 0\ 3\ 0$	$A_1\rightarrow A_2$	176.176	173.255	
	$G\rightarrow G$	176.186	173.263	178.1?
	$E_1\rightarrow E_1$	176.197	173.272	
	$E_3\rightarrow E_4$	176.197	173.272	
$1\ 0\ 0\rightarrow 1\ 1\ 0$	$A_3\rightarrow A_4$	185.592	182.847	
	$G\rightarrow G$	185.611	182.863	179.1
	$E_2\rightarrow E_2$	185.629	182.880	
	$E_4\rightarrow E_4$	185.629	182.880	
$1\ 1\ 0\rightarrow 2\ 1\ 0$	$A_4\rightarrow A_3$	171.937	170.398	
	$G\rightarrow G$	171.962	170.419	168.7
	$E_2\rightarrow E_2$	171.987	170.439	
	$E_4\rightarrow E_4$	171.987	170.439	
$0\ 0\ 0\rightarrow 0\ 0\ 1$	$A_1\rightarrow A_1$	398.661	396.727	
	$G\rightarrow G$	398.664	396.729	341.0
	$E_1\rightarrow E_1$	398.668	396.731	
	$E_3\rightarrow E_3$	398.668	396.731	

TABLE V. (*Continued.*)

$v\ v'\ v''\rightarrow v\ v'\ v''$[c]		MP2[b]	MP4[b]	Obs.
$0\ 0\ 1\rightarrow 0\ 1\ 1$	$A_1\rightarrow A_2$	199.151	196.820	
	$G\rightarrow G$	199.154	196.822	195.3
	$E_1\rightarrow E_1$	199.155	196.824	
	$E_3\rightarrow E_4$	199.149	196.824	
$0\ 1\ 1\rightarrow 0\ 2\ 1$	$A_2\rightarrow A_1$	202.482	202.515	
	$G\rightarrow G$	202.499	202.309	202.2
	$E_1\rightarrow E_1$	202.516	202.331	
	$E_4\rightarrow E_3$	202.522	202.331	

[a]In cm^{-1}.
[b]6-31G(d,p) basis set.
[c]v, v', and v'' are quantum numbers for the b_1, a_2, and a_1 modes.

method is inadequate for the treatment of the complex couplings between modes that display large amplitude motion. This is not too surprising in view of the extreme variation in the A^{ss} and A^{cc} coupling terms that are illustrated in Fig. 4.

The flexing of the COC bond angle as the methyl groups undergo internal rotation is responsible for the strong anharmonic interactions between the Q_7 bending mode and the overtone levels of the torsional Q_{15} mode that are observed in the infrared and Raman spectrum. The COC in-plane bending mode in DME-h_6 at 412.0 cm^{-1} lies between the A_1 overtone of the gearing and antigearing modes at 481.2 and 395.5 cm^{-1} and is in a position to interact through resonance perturbations. That this is indeed the case comes from the observation that the fundamental and the first sequence bands lie on top of each other in the spectrum, 241.0 and 240.2 cm^{-1}, respectively. The assignment of these infrared bands is confirmed by the double quantum 481.2 cm^{-1} Raman transition. The two-dimensional fully relaxed calculations with variable θ_1 and θ_2 are unable to account for the harmonic behavior of the first two intervals whereas the three-dimensional calculations satisfactorily reproduce the intervals at 241.2 and 239.7 cm^{-1}.
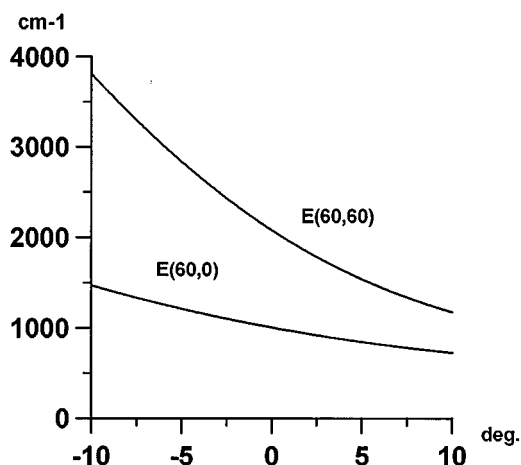

FIG. 3. The variation of the barrier maximum, $V(60°,60°)-V(0°,0°)$ and saddle points, $V(60°,0°)-V(0°,0°)$ as a function of the COC angle, α. α(equilibrium)$=110.949°$.
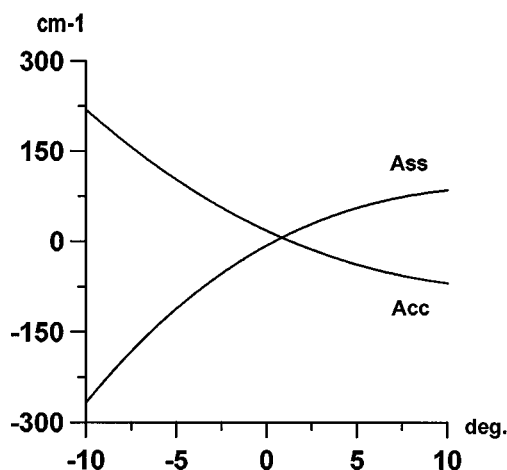
FIG. 4. The $\sin(3\theta_1)\sin(3\theta_2)$ and $\cos(3\theta_1)\cos(3\theta_2)$ coupling term as a function of the displacement of the COC bending angle from equilibrium. $A^{ss} = -6.9006 + 16.4074\alpha - 0.8460\alpha^2 + 0.0124\alpha^3$ and $A^{cc} = 17.8470 - 13.9243\alpha + 0.5744\alpha^2 - 0.0048\alpha^3$ (cm^{-1}).

The low lying A_3 and A_4 levels appear to be free from interactions with the COC bending level or the combinations with the torsional bands. For example, the $A_3(1,0,0) \rightarrow A_4(1,1,0)$ transition is calculated to lie at 226.2 cm^{-1}. It appears as the second strongest band in the far infrared (FIR) spectrum at 223.1 cm^{-1}. Likewise, the very strong band in the Raman spectrum at 450.5 cm^{-1} can be given the assignment $A_3(1,0,0) \rightarrow A_3(1,2,0)$ based on its calculated frequency 455.4 cm^{-1}.

The assignments of the fully deuterated compound -d_6 are also complicated by the resonance interactions from the bending mode. The perturbations in the spectra are very much larger than in the case of the -h_6 species. For example, the fundamental frequency in -d_6 is observed at 188.6 cm^{-1} and the first sequence at 195.3 cm^{-1}. Thus, the second interval unexpectedly increases. The reason for this increase is that the d_6/h_6 isotope shift is greater for the torsional modes than it is for the COC bending mode. The result is that the levels of the -d_6 compound are pushed closer together and the perturbations become stronger. Our calculations reverse the positions of the unperturbed levels of the -d_6 isotopomer and place the torsional gearing overtone level below the COC bending mode and thus the interaction pushes the levels in the wrong direction. As a result, the A_1 level of the COC bending mode is calculated to be too high and the first sequence of the gearing mode is too low. The solution to this problem would be to add additional modes of A_1 species into the model, that would have the effect of depressing the bending mode in the downwards direction and reversing the perturbation.

ACKNOWLEDGMENTS

[1] P. Groner, J. F. Sullivan, and J. R. Durig, *Vibrational Spectra and Structure*, edited by J. R. Durig (Elsevier/North-Holland, New York, 1981).
[2] (a) Y. G. Smeyers, M. L. Senent, V. Botella, and D. C. Moule, J. Chem. Phys. **98**, 2754 (1993); (b) D. C. Moule, Y. G. Smeyers, M. L. Senent, D. J. Clouthier, J. Karolczak, and R. H. Judge, *ibid*. **95**, 3137 (1991); M. L. Senent, D. C. Moule, Y. G. Smeyers, A. Toro-Labbe, and F. J. Penalver, J. Mol. Spectrosc. **164**, 66 (1994).
[3] M. L. Senent, D. C. Moule, and Y. G. Smeyers, Can. J. Phys. (in press).
[4] (a) Y. G. Smeyers, in *Advances in Quantum Chemistry*, edited by P. O. Lowden (Academic, New York, 1992), Vol. 24, pp. 1–77; (b) Y. G. Smeyers, in *Structure and Dynamics of Nonrigid Molecular Systems*, edited by Y. G. Smeyers (Kluwer, Dordrecht, 1994).
[5] Gaussian 92, M. J. Frisch, G. W. Trucks, M. Head-Gordon, P. M. W. Gill, M. W. Wong, J. B. Foresman, B. G. Johnson, H. B. Schlegel, M. A. Robb, E. S. Repongle, R. Gomperts, J. L. Andres, K. Raghavachari, J. S. Binkley, C. Gonzalez, R. L. Martin, D. J. Fox, D. J. Defrees, J. Baker, J. P. Steward, and J. A. Pople, Gaussian, Inc., Pittsburg PA, 1992.
[6] SPSS/PC+ 4.0, Advanced Statistics™, Chicago, Illinois.
[7] J. R. Durig, Y. S. Li and P. Groner, J. Mol. Spectrosc. **62**, 159–174 (1976).
[8] W. Neustock, A. Guarnieri, J. Demaison, and G. Wlodarczak, Z. Naturforsch **45a**, 702 (1990).
[9] P. Groner and J. R. Durig, J. Chem. Phys. **66**, 1856–1874 (1977).